Simultaneous evaluation of the enantiomeric and carbon isotopic ratios of *Cannabis sativa* L. essential oils by multidimensional gas chromatography

Lorenzo Cucinotta[1,2], Gemma De Grazia[1], Giuseppe Micalizzi[1], Luana Bontempo[3], Federica Camin[2,4,5], Luigi Mondello[1,6,7], Danilo Sciarrone[1*]

[1]*Department of Chemical, Biological, Pharmaceutical and Environmental Sciences, University of Messina, 98168 Messina, Italy*

[2]*Department of Food Quality and Nutrition, Research and Innovation Centre, Fondazione Edmund Mach, via Mach 1, 38098 San Michele all'Adige (TN), Italy*

[3]*Food Quality and Nutrition Department - Traceability Unit, Fondazione Edmund Mach, via Mach 1, 38098 San Michele all'Adige (TN), Italy*

[4]*Center Agriculture Food Environment (C3A), University of Trento, Via Mach 1, 38010 San Michele all'Adige, (TN), Italy*

[5]*International Atomic Energy Agency, Vienna International Centre, PO Box 100, A-1400 Vienna, Austria.*

[6]*BeSep s.r.l., c/o Department of Chemical, Biological, Pharmaceutical and Environmental Sciences, University of Messina, 98168 Messina, Italy*

[7]*Chromaleonts.r.l., c/o Department of Chemical, Biological, Pharmaceutical and Environmental Sciences, University of Messina, 98168 Messina, Italy*

*Corresponding author. Prof. Danilo Sciarrone

Tel. +39-090-6766463; fax +39-090-358220. *E-mail address*: dsciarrone@unime.it

Key words: Multidimensional gas chromatography, enantio gas chromatography, isotopic ratio mass spectrometry, *Cannabis sativa* L., chiral terpenes

Abstract

Recent times have witnessed an upsurge of interest in hemp and hemp-derived products, as driven by the scientific findings specific to the pharmacological properties of *Cannabis sativa* L. and its constituents. There has been evidence that the terpene profile, along with the cannabinoid content, produces in humans the effects associated with different strains, beyond fragrance perception. A great deal of effort has been put in developing analytical approaches to strengthen the scientific knowledge on cannabis essential oil composition and provide effective tools for ascertaining the authenticity of commercial cannabis samples. To this concern, enantio-GC-C-IRMS has proven to be effective in providing useful data for assessing the ranges characteristic of the genuine samples and detect any fraudulent additions. This research aimed at providing for the first time the enantiomeric and isotopic ratios of target terpenes in cannabis essential oils, obtained from microwave-assisted hydro-distillation from the fresh and dried inflorescences of different cannabis varieties. Implementing multidimensional gas chromatography separation was mandatory prior to detection, in order to obtain accurate $\delta^{13}C$ and enantiomeric data from completely separated peaks. For this purpose, a heart-cut method was applied, based on the coupling of an apolar first dimension column to a secondary chiral cyclodextrin-based stationary phase. Afterwards, the data gathered from MDGC-C-IRMS/qMS analysis of a set of genuine samples were used to evaluate the quality of nineteen commercial cannabis essential oils purchased from local stores. Remarkably the data in some cases evidenced enantiomeric and $\delta^{13}C$ ratios outside the typical ranges of genuine oils. Such findings suggest the usefulness of the method developed to ascertain the genuineness and quality of cannabis essential oils.

1) Introduction

Cannabis is an herbal annual plant, for which research has long been limited because of legal restrictions across the 20th and the beginning of the 21st century, due to its renowned psychotropic activity and the related illicit use. From a normative point of view, the cultivation has been promoted in Europe only in the last decade, specifically for those varieties, e.g *Cannabis Sativa* L., with content in tetrahydrocannabinol <0.2% [1]. As a consequence of the increased scientific interest, nowadays hemp market and the linked manufactures are ever spreading. Among the products derived from *Cannabis Sativa* L., the essential oil obtained by the inflorescences is one of the most distinctive, due to the harmonious balance between the main monoterpene and sesquiterpene components along with their oxygenated derivatives [2]. Cannabis chemical composition may vary in relation to the inflorescence being fresh or dry [2], its variety, and the extraction methodology used. In the last decades, steam distillation or hydro-distillation [3] have been the most used techniques for oil extraction, as well as the innovative microwave assisted hydrodistillation apparatus [4-5]. Thanks to the latest approach, it was possible to carry out hydro-distillation of the hemp inflorescences, and maximize the final yield by finely tuning some instrumental parameters, such as microwave power and time program [5]. Alongside genuine oils obtained from the inflorescences, also reconstituted oils, obtained by natural or synthetic sources, are nowadays more and more present on the market. Most of them are declared to contain the typical hemp terpene compounds, such as α-pinene, myrcene and (E)-β-caryophyllene, aiming to emulate the flavor and other properties of natural cannabis oils. Yet, no reference data are reported in the literature about the chemical composition of these oils. In this regard, gas chromatography coupled to flame ionization detector (GC-FID) and to mass spectrometry (GC-MS) are well suited techniques for investigation of the qualitative and quantitative composition of these oils in terms of volatile components. However, there is no chance to highlight the differences with respect to extracted genuine oils, by these means. The employment of more sophisticated analytical techniques is needed to tackle such a task. Enantio selective gas chromatography (Es-GC) has historically played a key role for the authenticity assessment of natural essential oils, proving to be one of the most effective analytical approaches for these purposes [6]. In fact, chiral compounds show typical enantiomeric ratios in natural samples, being the metabolites of specific biochemical pathways of the plant of origin, exerting a critical role for the plant defense from external attacks. By these means, the presence of unusual enantiomeric excesses for a given sample has often allowed unveiling fraudulent additions by comparison to genuine reference values, using monodimensional and multidimensional GC systems [7-9]. Conversely, nowadays key chiral components can be selected by natural sources having identical or similar enantiomeric ratios with respect to the sample investigated [10], thereby reducing the possibility to detect any differences deriving from adulterations. In such cases, additional analytical techniques are needed to highlight further typical traits of the plant of origin. Gas chromatography coupled to isotope ratio mass spectrometry (GC-C-IRMS) is

equally broadly recognized as a suitable technique to assess the origin and genuineness of a sample. A GC-C-IRMS method can provide crucial information about the natural, synthetic or biosynthetic origin of specific compounds in a sample, allowing in many cases to unveil fraudulent practices. Since the distribution of carbon stable isotopes strictly depends on the photosynthetic carbon metabolism and the geographic origin of the plant, the evaluation of the $\delta^{13}C$ isotopic value of key volatile compounds represents a powerful tool for genuineness assessment [11-13]. It is straightforward that a combined approach consisting of Es-GC-C-IRMS would allow for the simultaneous evaluation of both chiral and $\delta^{13}C$ isotopic ratios, thus enabling to detect fraudulent additions to genuine oil samples. The coupling of chiral separation and IRMS detection was first demonstrated by Mosandl *et al.* [14] for the differentiation of biotechnological and synthetic γ-decalactone, and later by few more authors [15-18]. Although representing a powerful tool for authenticity assessment, this approach suffers from important drawbacks, which have greatly limited its widespread diffusion. When dealing with medium-to-high complex samples, incomplete separation of the compounds of interest may occur, due to insufficient chromatographic resolution. Within crowded zones across a chromatogram, the presence of closely retained compounds in addition to their enantiomers, may lead to co-elutions; this would in turn result in wrong evaluation of the enantiomeric and isotopic ratios. Chiral compounds can be resolved into their enantiomers on a suitable stationary phase, and in the presence of further co-elutions, the enantiomeric ratios can be still calculated by extracting specific *m/z* ions. On the other hand, this problem would negatively impact the $\delta^{13}C$ isotopic ratio evaluation, due to the uneven distribution of carbon isotopes (^{12}C and ^{13}C) along the CO_2 peak [19-20]. A slightly different retention is observable for the same molecules containing different amount of the two isotopes. In fact, different Van der Waals dispersion forces during solute/stationary interaction cause an enrichment in the heavier isotope of the initial part of the peak, while the lighter isotope will be more represented in the final part of the peak. Thus, shifted isotopic values will be observed with respect to those of a pure peak [19-20], depending on which part of the peak is co-eluted. If the co-elution affects the front of the peak, a more negative $\delta^{13}C$ value will be observed; on the contrary, a more positive $\delta^{13}C$ value will be measured if the tail of the peak of interest is affected by co-elution. In the case of a complete co-elution, no MS "tricks" may be used, due to the conversion of both the components to CO_2. In this case, evidence of such a situation would be only obtained by checking the CO_2 ratio differentiation [20]. Under these circumstances, multidimensional gas chromatography exploited in the heart-cut mode (HC-MDGC) may represent the technique of choice, thanks to the higher peak resolution afforded by the coupling of two full-length columns with different selectivity [21]. In the literature, only few works employed a MDGC system before the IRMS detection, and among these only one deals with the detection of enantiomers [17]. In this research, an Es-MDGC-C-IRMS/qMS method was developed, by employing an apolar column as the first dimension (^1D) and a chiral cyclodextrine-based stationary phase as the second dimension (^2D), to evaluate the enantiomeric and isotopic ratios of well separated target

terpenes in cannabis oils, for the first time. A microwave assisted hydro-distillation (MAHD) method earlier described by Micalizzi *et al.* [5] was adopted to obtain in-house genuine oils from the fresh and dried inflorescences of different cannabis varieties. In parallel, commercial oils declared as reconstituted or natural were analyzed, and the results were compared to those obtained for the genuine samples extracted in-house. To the best of our knowledge, this is the first time that $\delta^{13}C$ ratios are provided for the terpene fraction of *Cannabis sativa* L. essential oil samples. The data gathered from analysis of the different sample varieties were used to establish the characteristic enantiomeric and isotopic ranges of Cannabis sativa L. essential oil.

2) Experimental section

2.1 Sample preparation

Fifteen dry hemp inflorescences belonging to Futura 75, Kompolti, Felina 32, Tisza and CS (Carmagnola Selezionata) varieties and one fresh hemp inflorescence belonging to Futura 75, registered in the EU Plant variety database [22], were provided by the Canapar group, Ragusa, Italy. Nineteen commercial hemp oils, 16 reconstituted and 3 declared as naturals, were purchased from local stores. All the samples were diluted 1:10 in *n*-hexane before the GC run. A C_7-C_{30} *n*-alkane mix, kindly provided by Merck Life Science (Darmstadt, Germany), was used for the calculation of linear retention index (LRI) values. In order to calibrate the measured $\delta^{13}C$ values to the VPDB scale, the CO_2 reference gas was calibrated using four reference compounds, namely iodomethane ($\delta^{13}C$ -54.59‰) and three alkanes from the Indiana mix A7, i.e. hexadecane ($\delta^{13}C$ -26.15‰), octadecane ($\delta^{13}C$ -32.70‰) and eicosane ($\delta^{13}C$ -40.91‰) (Indiana University, Bloomington, IN). Isotopic ratio measurements of the samples of interest were made by the following formula:

$$\delta^{13}C = \frac{Rsample - Rstandard}{Rstandard}$$

where *R* represents the abundance ratio of the heavier carbon isotope against the lighter one ($^{13}C/^{12}C$).

All the samples were stored at +4 °C.

2.2 Instrumental parameters

2.2.1 Microwave-assisted-hydro-distillation (MAHD) conditions

Six hundred mL of ultrapure water were added to 200 g of inflorescence, and the biomass was uniformly mixed. The resulting mixture was placed inside a 2 L ETHOS-X glass reactor and thus into a Milestone "Ethos X" extractor

142 (Milestones, Sorisole, Italy), under previously optimized conditions [5]. Once the run was completed, essential oils
143 were collected from the distillation system.

144

145 **2.2.2 MDGC-C-IRMS/qMS conditions**

146 The MDGC-C-IRMS/qMS prototype consisted of an AOC-20i autosampler, two GC-2010 Plus gas chromatographers
147 (defined as GC1 and GC2), connected by means of a heated transfer line (Shimadzu Europa, Duisburg, Germany). GC1
148 was equipped with a split/splitless injector, a flame ionization detector (FID) and a Deans-switch (DS) transfer device,
149 connected to an advanced pressure control unit (APC), which supplied the same carrier gas (He) (Shimadzu Europa,
150 Duisburg, Germany) allowing to divert the first column eluent to the FID or to the second column in the GC2. The latter
151 was hyphenated in parallel to a QP2010 Ultra quadrupole mass spectrometer (Shimadzu Europa, Duisburg, Germany)
152 and to a VisION IRMS system by means of a GC V furnace system (Elementar Analysensysteme GmbH,
153 Langenselbold, Germany) maintained at 850 °C. The split/splitless injector was maintained at 280 °C, at a split ratio
154 10:1, delivering to the ^{1}D column, an SLB-5 ms 30 m × 0.25 mm i.d. × 0.25 μm df (Merck Life Science, Darmstadt,
155 Germany), a constant helium flow of 1.0 mL/min. A pressure program was used, from 185 kPa (7 min) to 247 kPa (5
156 min) at 1.89 kPa/min, to 300 kPa at 1.89 kPa/min and finally to 330 kPa at 9.48 kPa/min. The GC1 oven was ramped as
157 follows: 50 °C (7 min) to 227 °C at 3 °C/min with an isotherm at 150 °C (5 min), finally to 280 °C at 15 °C/min. The
158 FID (330 °C; H_2 flow, 40.0 mL/ min; air flow rate, 400 mL/min; sampling rate, 80 ms equal to 12.5 Hz) was connected
159 to the DS device via a 0.25 m × 0.18 mm i.d. stainless steel uncoated column and used to monitor the ^{1}D eluent. GC2
160 was equipped with a MEGA-DEX ASX 1 chiral column 25 m × 0.25 mm i.d. × 0.25 μm df (MEGA, Milano, Italy), and
161 the temperature was ramped as follows: 40 °C (22 min) to 76 °C (5 min) at 2 °C/min, to 145 °C at 3 °C/min and finally
162 to 195 °C at 8 °C/min. The ^{2}D column was connected at one side to the DS device and at the other side to a zero dead-
163 volume tee-union (Valco). The effluent was split to the combustion chamber and to the IRMS system via a 0.85 m ×
164 0.25 mm i.d. uncoated column and to the qMS via a 2 m × 0.1 mm i.d. uncoated column. A pressure program was
165 applied to the APC device in order to maintain a constant carrier flow also in the ^{2}D column (≈1 mL/min): 140 kPa (22
166 min), to 165 kPa (5 min) at 1.39 kPa/min, to a final pressure of 210 kPa at 1.39 kPa/min. The qMS ion source and
167 interface temperature were maintained at 200 °C; the mass range 40-400 *m/z* was monitored at an acquisition speed of
168 10 Hz. The target compounds were identified by searching their qMS spectra against the FFNSC 4.0 mass spectral
169 library database (Shimadzu Europa, Duisburg, Germany), using a double filter based on spectral similarity and Linear
170 Retention Index (LRI). The VisION IRMS (Elementar Analysensysteme GmbH, Langenselbold, Germany) was a bench
171 top 5 kV system equipped with an integrated monitoring gas delivery system. The combustion chamber was provided

with a high performing silicon carbide tube furnace for the quantitative, fractionation-free conversion of the compounds to pure gases (CO_2 and H_2O). The CO_2 produced by pyrolisis of each component was transferred to the IRMS, while the water produced was removed through a nafion membrane. The system was designed with reduced dead volumes to maintain the chromatographic integrity of the separated compounds, preserving the chromatographic resolution at the IRMS. An auxiliary He line (sample line He), automatically controlled through a second channel of the APC unit, was used in the furnace to allow a proper control over the open split conditions for the IRMS. The following settings were applied to the VisION system: acceleration voltage, 3795.007 V; trap current, 600.000 μA; magnet current, 3700.000 mA. The APC was operated in constant flow mode, to maintain the open split in a steady state. An electron-impact ionization (EI) gas source, a variable field, stigmatically focused electromagnet for beam separation and multi-channel Faraday collectors for beam detection were used. IRMS data were collected by IonOS stable isotope data processing software ver. 3.0.0.5196 (Elementar Analysensysteme GmbH, Langenselbold, Germany); the apex track integration method was exploited to automatically find the correct starting and finishing point of the peaks. All the analyses were led at least in triplicate and standard deviations for IRMS measurements were found to be under < 0.5.

3. Results and discussion

3.1 Extraction of the cannabis oil samples by microwave-assisted hydrodistillation (MAHD)

Aiming to evaluate the isotopic and enantiomeric profile of the cannabis volatile fraction, MAHD extraction was applied to sixteen genuine samples consisting of fresh and dry hemp inflorescences. By the employment of a microwave-assisted system, heat was applied to the soaked biomass to facilitate the break of the oileferous glands and the release of essential oil. By this method, the first drops of essential oil fell after about 5 min of distillation at 1200 W, at a temperature around 94 °C. The samples selected for extraction are listed in Table 1. One sample was obtained by fresh hemps of Futura 75 (Sample 1), while the other dry samples belonged to other varieties: 9 of Futura 75 (samples 2-10), 2 of Felina 32 (samples 11-12), 1 of Tisza (sample 13), 2 of Kompolti (samples 14-15) and 1 of CS (Carmagnola Selezionata) (sample 16). Unfortunately, the high cost and the difficulties in retrieving genuine plant material for oil extraction have limited the number of oil samples included in this research. This represents a common issue for studies focused on ascertaining of the genuineness ranges, since they involve investigation of natural samples in order to assess the characteristic $\delta^{13}C$ and enantiomeric ratios. The limited size of samples available prevented from obtaining statistical significant results in this study, on the differences among the distinct Cannabis sativa varieties. Nonetheless the data gathered from analysis of the essential oil samples were used to establish the characteristic ranges of the enantiomeric and isotopic ratios of *Cannabis sativa* L.

ID	Varieties	Fresh/dry	Origin
1	Futura 75	fresh	Italy
2	Futura 75	dry	Italy
3	Futura 75	dry	Italy
4	Futura 75	dry	Italy
5	Futura 75	dry	Italy
6	Futura 75	dry	Italy
7	Futura 75	dry	Italy
8	Futura 75	dry	Italy
9	Futura 75	dry	Italy
10	Futura 75	dry	Croatia
11	Felina 32	dry	Italy
12	Felina 32	dry	Italy
13	Tisza	dry	Italy
14	Kompolti	dry	Italy
15	Kompolti	dry	Italy
16	CS (Carmagnola selezionata)	dry	Italy

Table 1. Cannabis varieties selected for essential oil extraction from hemp inflorescences.

3.2 **Monodimensional Es-GC-C-IRMS/qMS approach**

Es-GC-C-IRMS/qMS analyses were initially carried out in order to determine both the enantiomeric and isotopic ratio of the genuine cannabis oils. To this purpose, a chiral column MEGA DEX-ASX-1 proved to be a suitable stationary phase, due to its capability to efficiently separate the target enantiomers before the IRMS determination. Nevertheless, for the main chiral terpens, a number of issues arose in the monodimensional chiral analysis of some genuine cannabis oils, as shown in **Fig. 1A** for a Futura 75 essential oil. As can be easily noticed, although α-pinene and β-pinene enantiomers were efficiently separated in the Es-GC-C-IRMS/qMS profile, co-elutions occurred with other achiral components. In the case of (+)-α-pinene, present in higher amount with respect to heptanal, the partial peak overlapping might have a limited influence on the peak area evaluation for the enantiomeric ratio assessment and on the $\delta^{13}C$ evaluation [20]. Otherwise, the co-elution occurring between (+)-β-pinene and another major compound (e.g. myrcene), introduces a critical issue. In this case, the incomplete separation strongly influenced both the enantiomeric and isotopic ratio evaluation that clearly could not be achieved in an accurate manner. Concerning the enantiomeric ratio evaluation, the use of simultaneous qMS detection would in principle allow to resolve the chromatographic coelution by monitoring the extracted *m/z* ions of the compounds of interest. Unfortunately, in the case of monoterpene compounds, the respective EI MS spectra will be characterized by the same fragmentation pattern and show nearly identical fragment ions, thus the use of this approach is precluded. From the IRMS standpoint, a similar approach cannot be envisaged,

since all the organic matter has to be converted to CO_2 before the $\delta^{13}C$ determination, with a consequent loss of any structural information of the analytes [19]. As a consequence, the occurrence of a co-elution involving the right part (tail) of the peak is expected to cause a relevant positive shift of the $\delta^{13}C$ value, as for the case of (+) β-pinene, due to the depletion of the $^{44}CO_2$ fragment (lower amount of β-pinene molecules containing ^{12}C). **Fig. 1B** shows a further co-elution in a Futura 75 oil, involving the (-)-limonene enantiomer which is partially coeluted with (E)-β-ocimene. In this case, being the latter a higher abundant compound, a wrong estimation of the $\delta^{13}C$ value should be expected, unlike the case of (+)-α-pinene discussed above. Moving forward in the chromatogram, further critical cases may be observed in the sesquiterpene elution zone of a Kompolti sample (**Fig. 1C**). Selina-3,7(11)-diene and of selina 4-(15), 7(11)-diene compounds were successfully separated into their enantiomers; nevertheless the late eluting enantiomer of selina 4-(15),7(11)-diene and the first eluting enantiomer of selina-3,7(11)-diene overlap with an interfering peak, namely Germacrene B. Likewise, unreliable results may be predicted in this case, notably a more positive $\delta^{13}C$ value for selina 4-(15),7(11)-diene and a more negative $\delta^{13}C$ value for selina-3,7(11)-diene, with respect to their true values.

Please insert here Fig.1

Fig. 1: *Es-GC-C-IRMS/qMS analysis showing the co-elutions of: (+)–α-pinene and (+)–β-pinene peaks (A) and (-)-limonene peak (B) in a Futura 75 essential oil, the enantiomers of selina diene isomers in a Kompolti essential oil (C)*

3.3 Monodimensional GC-C-IRMS/qMS approach

Inaccurate results were also obtained by the GC-C-IRMS/qMS analysis, performed on an apolar column. As can be seen in **Fig. 2**, co-elutions affected the peaks of the target oil compounds in the monoterpene and sesquiterpene zone. **Fig. 2A** shows a partial co-elution involving limonene and eucalyptol in a Futura 75 sample: due to their similar LRIs on an apolar stationary phase (1030 and 1032 respectively), a partial overlap occurred, again generating unreliable results for the $\delta^{13}C$ values.

Please insert here Fig. 2

Fig. 2: *GC-C-IRMS/qMS analysis showing the co-elutions of: limonene and eucalyptol peaks (A) and selina 4-(15), 7(11)-diene and (E)-α-bisabolene peaks (B) in a Futura 75 essential oil.* $^{45/44}CO_2$ *ratio differentiation (IRMS: upper trace) and extracted ion chromatogram (qMS: lower traces) of selina 4-15, 7(11)-diene peak (C)*

Fig. 2B shows the critical case of selina 4-(15),7(11)-diene, identified by exploiting double-filtered MS search based on mass spectral similarity (> 90%) and LRI (± 5 units window). Due to its Gaussian shape, it would have been regarded as a pure peak, at first sight. Yet, a deeper investigation by monitoring the MS spectrum along the peak highlighted the

presence of co-eluted (E)-α-bisabolene in the peak tail. In fact, both components were characterized by the same LRI 1540 on an apolar column. In addition, **Fig. 2C** shows how this coelution can be revealed by monitoring two different extracted ions from the MS total ion current (TIC) (lower trace) and by $^{45/44}CO_2$ ratio differentiation for the IRMS (upper trace). In detail, *m/z* 93 and *m/z* 105 were extracted from the TIC, being *m/z* 93 the base peak for (E)-α-bisabolene and *m/z* 105 > *m/z* 93 for selina 4-(15),7(11)-diene. The higher amount of the *m/z* 93 ion in the tail of the peak clearly confirm the presence of (E)-α-bisabolene at this level, further confirmed by the unusual $^{45/44}CO_2$ ratio differentiation reported in the upper profile. At this point it was clear the need to implement a multidimensional approach to increase the separation capability.

3.4 Multidimensional Es-GC-C-IRMS/qMS approach

3.4.1 System configuration

Different MDGC approaches are reported in the literature exploiting both single and double oven configurations. Apart from the economical aspect, the technical advantage of a double oven configuration relies on the capability for separate temperature program optimization for each of the columns employed. Such an instrument configuration requires the coupling of a GC-MS to a GC-FID system via a heated transfer line. Usually, since in a GC-MS system the spectrometer is located on the left side of the GC, the transfer line connecting to the (second) GC-FID instrument is located on the right side (**Online resource 1**). In such configuration, the GC-FID system is regarded as the first chromatographic dimension (^{1}D) and thus the GC-MS system as the second one (^{2}D). In this research, given the need for splitting the second column eluate between the qMS and IRMS systems, an inverted configuration was chosen, in which the IRMS system was located on the right side of the MDGC system (**Online resource 2**). Hence, the primary column (^{1}D) and the DS device were located by the GC-MS side while the secondary column, connected to the DS, was passed through the heated transfer line and located by the GC-FID system. The latter was provided with a T-union located in the oven, connected at one side to the (^{2}D) outlet and at the other side to two retention gaps differing in length and I.D. and directed to the two spectrometers. The configuration here described was chosen on the basis of the required split ratio of about 1:10 to the qMS and IRMS system, respectively. It is in fact well known that IRMS detection suffers from the low natural abundance of the ^{13}C isotope that is about 1% of the ^{12}C isotope, leading to a proportional reduction of the sensitivity achievable. To compensate for this, a higher resistance was required to the qMS system, obtained via a 2 m x 0.1 mm I.D. retention gap, and a lower resistance was needed to the IRMS side. In order to minimize dead volumes and preserve the chromatographic resolution, the shortest retention gap length able to provide the demanded split ratio was selected, namely a 0.8 m x 0.32 mm I.D. The inverted configuration here described allowed for positioning the T-union as close as possible to the IRMS system, by means of a shorter retention gap.

3.4.2 Selection of the peaks of interest after ^{1}D stand-by analysis

In order to overcome the limitations discussed in section 3.3, an MDGC method was implemented, as front-end separation before simultaneous qMS and IRMS detection. In detail, an apolar SLB-5ms column was employed as ^{1}D and the chiral MEGA DEX-ASX-1 as ^{2}D. The first step of any HC-MDGC analysis involves the identification of the peaks of interest after a ^{1}D analysis performed in the stand-by mode (no heart-cuts selected). Since no qualitative information were available after the ^{1}D detector (FID), the identity of each peak of interest was confirmed on the basis of the elution order observed in monodimensional GC-MS analysis on the same stationary phase. Furthermore, the experimental LRIs of the peaks obtained after a ^{1}D stand-by analysis were matched to the theoretical values, within a ±10 units tolerance (**Online resource 3 and 4**) [23]. Cannabis oil samples and an alkane homologous series C_7-C_{30} were analyzed within the same instrumental parameters and the experimental LRIs were calculated by the following formula:

$$LRIx = \frac{100n + 100(t_R x - t_R n)}{(t_R n + 1 - t_R n)} \quad (eq.\ 1)$$

where n and $t_R n$ are the carbon number and retention time of the alkane eluted before the peak of interest and $t_R n + 1$ the retention time of the alkane eluted after the peak of interest.

3.4.3 Multidimensional Es-GC-C-IRMS/qMS analysis

The oil samples were subjected to a multidimensional separation approach prior to determine the isotopic and enantiomeric ratios of the peaks of interest. **Fig. 3** shows the ^{1}D FID chromatogram of a cannabis essential oil acquired in the stand-by mode (black trace). Among the main chiral terpenes, a total of nine compounds were selected for the heart-cut, for further separation on the ^{2}D chiral column: α-pinene, β-pinene, limonene, linalool, α-terpineol, (E)-β-caryophyllene, selina 4(15),7-11-diene and selina 3,7(11)-diene and (E)-β-caryophyllene oxide. Minor chiral components, namely camphene, borneol, fenchyl alcohol and (E)-nerolidol, were not taken into consideration due to their low amount in the oils. As shown in Table 2, their experimental LRI values (LRI_{exp}) ranged within ± 5 units with respect to the theoretical data (LRI_{theor}).

Peak ID	*Compound*	LRI_{theor}	LRI_{exp}
1	α-pinene	933	935
2	β-pinene	978	980
3	limonene	1030	1032
4	linalool	1101	1103
5	α-terpineol	1195	1200
6	(E)-β-caryophyllene	1424	1427

7	selina 4(15),7-11-diene	1540	1544
8	selina 3,7(11)-diene	1546	1550
9	(E)-β-caryophyllene oxide	1587	1591

Table 2. *The theoretical and experimental LRI values calculated for a ^{1}D stand-by analysis of a Kompolti oil.*

A heart-cut window was then selected, for each compound to be transferred to the second chiral column in the "cut" mode (Pink trace in **Fig. 3**).

Please insert here Fig. 3

Fig 3. *^{1}D stand-by (black chromatogram) and cut (pink chromatogram) FID analysis of a Cannabis Sativa L. essential oil. Cut windows: I: α-pinene, II: β-pinene, III: limonene, IV: linalool, V: α-terpineol, VI: (E)-β-caryophyllene, VII: selina 4(15),7-11-diene and selina 3,7(11)-diene, VIII:* (E)-β-*caryophyllene oxide*

The combination of two chromatographic separation mechanisms allowed overcoming the issues inherent to the monodimensional analysis; not only a satisfactory separation was achieved for each of the enantiomeric compounds transferred, but also all co-elutions of the latter with achiral sample components were prevented. **Fig. 4** shows different zoomed zones of the chromatogram, illustrating the improved separation afforded for each enantiomer by the multidimensional approach. In detail, **Fig. 4A** shows the separation of α-pinene, β-pinene and limonene enantiomers, while in the monodimensional GC-C-IRMS analysis heptanal, myrcene, (E)-β-ocimene and eucalyptol were co-eluted among these chiral compounds. **Fig. 4B** shows the results for linalool and α-terpineol enantiomers. **Fig. 4C** shows the (E)-β-caryophyllene peak separated from γ-elemene, obviously co-eluted on the apolar ^{1}D column due to the very close LRI values (1424 *vs* 1432) and to the high amount of caryophyllene in the sample. Concerning the selina diene isomers, the separation of the four enantiomers is evident in the same chromatogram, free from overlapping with Germacrene B and (E)-α-bisabolene peak, which were coeluted with selina 4-(15), 7(11)-diene in the monodimensional separation on the chiral and achiral column, respectively (see **Fig.1** and **Fig. 2**).

Please insert here Fig. 4

Fig. 4. *MDGC profile of the target monoterpenes in a Futura 75 (A) and a Felina 32 (B) essential oil samples and of the target sesquiterpenes in a Futura 75 essential oil sample (C)*

In the MDGC approach only a minor co-elution was observed between the second eluting selina 4-(15), 7(11)-diene peak and the first eluting peak of selina 3,7(11)-diene enantiomers. Unfortunately, no data are available about the

328 elution order of these enantiomers. Finally, the separation of the two enantiomers of (E)-β-caryophyllene oxide was
329 achieved in dried hemp inflorescence samples, thanks to the higher amount of this compound generated by oxidation
330 occurring during drying [5]. By the optimized Es-MDGC-C-IRMS/qMS method, it was possible to obtain in a single
331 analysis the enantiomeric and isotopic ratio data of all the sample components simultaneously, which are reported in
332 Table 3.

333 **Table 3. Enantiomeric and isotopic ratio data of genuine *Cannabis Sativa* L. oils**

334 Clear differences were found in the qualitative and quantitative composition in monoterpenes and sesquiterpene, as
335 related to the type of inflorescence and the variety itself [2,5]. Moreover, characteristic enantiomeric and isotopic ratios
336 were found for the target compounds in all the sixteen genuine oils analyzed. The enantiomeric ratio observed for all the
337 natural samples were in good agreement with respect to the literature data [4-5], although in this research a higher
338 number of samples were investigated. A marked preponderance was observed in all the hemp varieties for (+) α-pinene
339 (93.38-97.08%), (+) β-pinene (78.56-88.03%) and for (-)-(E)-β-caryophyllene oxide (91.67-98.95%). An important
340 variability was observed for limonene and α-terpineol, which can exceed both in the dextrorotatory and levorotatory
341 forms. Among the linalool enantiomers the dextrorotatory form was predominant in all the varieties investigated (57.76-
342 74.90%). Last, in the case of selina diene isomers it was observed a racemic behavior or, being not known the elution
343 order of the two enantiomers, a slightly predominance of the late eluted enantiomers for both the 4(15) and 3(11)
344 isomers. Concerning the (E)-β-caryophyllene enantiomers, the occurrence of the levorotatory form at nearly 100% is
345 widely reported in the literature, and the data acquired for the samples analyzed were also in accordance with this
346 literature finding [4-5]. Dealing with the isotopic distribution, differences were observed in terms of $\delta^{13}C$ in relation to
347 the specific varieties, as reported in Table 3. Thanks to the chiral separation achieved, the $\delta^{13}C$ ratios of the pure
348 enantiomer peaks were measured. In some cases, especially for low concentrated components and depending on the
349 enantiomeric ratio, or in the case of incomplete peak separation, only one enantiomer was measured. A linearity test
350 automatically performed by the system showed a consistent $\delta^{13}C$ ratio (within the uncertainty of the instrument signal)
351 in the response interval above 0.5 nA, thus signals below this threshold were not taken in consideration. Even if the
352 coupling of chiral chromatography to IRMS detection has been overlooked in the last decades, according to the few
353 literature data available, no significant $\delta^{13}C$ ratio differences should be expected within enantiomers of the same
354 molecule [14-18]. For all the successfully separated enantiomers, $\delta^{13}C$ ratio values were measured after the ^{2}D
355 separation. In general, more negative $\delta^{13}C$ ratios were found for samples 13-16 (Tisza, Kompolti, and Carmagnola
356 Selezionata) with respect to samples 1-10 (Futura 75) and 11-12 (Felina 32). Focusing on the Futura 75 samples, it was
357 possible to highlight some isotopic differences between oils of different origin, namely from Italy (samples 1-9) and

Croatia (sample 10), which can be appreciated in **Fig. 5A**. Sample 10 showed more negative $\delta^{13}C$ ratios with respect to samples 1-9. In this case, considering the genuineness of the Croatian oil, to avoid the isotopic discrimination due to the geographical origin, an isotopic internal standard (i-ISTD) was introduced, as reported by Mosandl *et al* [16]. In this concern, (-)-(E)-β-caryophyllene was chosen as i-ISTD, being one of the characteristic compound in cannabis essential oil and biogenetically related to the other compounds under investigation. **Fig. 5B** shows how the use of the internal standard approach allowed confirming the genuineness of all the Futura samples, regardless of their origin.

Please insert here Fig. 5

Fig. 5. *(A) Comparison between Italian Futura 75 $\delta^{13}C_{VPDB}$ range (samples 1-9) and Croatian Futura 75 sample (sample 10); (B) comparison after the employment of an isotopic-ISTD*

In the case of the two selina diene isomers, the small co-elution occurring at the peak base between the second eluted enantiomer of the 4(15), 7(11) and the first eluted enantiomer of the 3, 7(11) isomers was negligible to the aim of enantiomeric ratio evaluation. Yet, such a small lack of separation would significantly affect the $\delta^{13}C$ evaluation in all the samples analyzed. A representative example was illustrated by the values measured for the Futura 75 oil (sample 10). Among the four peaks corresponding to the enantiomers of selina diene isomers, baseline separation was achieved only for the first (4(15), 7(11)) and the fourth (3, 7(11)) peaks, thus it could be assumed that the $\delta^{13}C$ ratios determined for these two compounds were accurate values. On the other hand, being the second and third peaks co-eluted to a very small extent, no significant differences were in principle foreseeable. Conversely, for the second eluted selina diene 4(15), 7(11) enantiomer a more positive $\delta^{13}C$ ratio was measured, with respect to the first eluted enantiomer (*viz.*, -27.2 *vs* -29.3‰). Whilst, the same discrepancy, but with an opposite trend, was observed for the first eluted selina diene 3,7(11) enantiomer, which showed a more negative $\delta^{13}C$ ratio with respect to the second eluted enantiomer (*viz.*, -32.0 *vs* -29.4‰). These findings are in agreement with what discussed earlier about isotopic fractionation due to the chromatographic effect, with opposite trends for co-elutions affecting the initial (front) or final (tail) part of a peak. For this reason, the $\delta^{13}C$ ratios of these two compounds are not reported [11,19,20].

3.4.4 Analysis of commercial samples

Nineteen commercial cannabis essential oils purchased from local stores were analyzed. Among these, three oils were declared as genuine, while the remaining as were labelled as reconstituted. The enantiomeric and $\delta^{13}C$ ratios obtained are shown in Table 4. Among the three commercial oils labeled as genuine, all the samples showed chiral and isotopic behavior similar to those of a genuine sample.

Please enter here table 4

Table 4. Enantiomeric and $\delta^{13}C$ ratios obtained for the commercial *Cannabis Sativa* L. oils, and their origin as declared on the label.

Most chiral and isotopic ratios determined for the reconstituted oil samples were outside the ranges observed for the genuine samples. In some oils, the terpene fraction was represented mainly by α-pinene and β-caryophyllene, as in the case of samples 1-5, while the other analytes were found in very low concentrations or were absent. In detail, the enantiomeric ratios in all the reconstituted samples fell outside the range of genuineness: (-)-α-pinene enantiomer was > 70% in samples 1-8, and close to racemic values for samples 9-16, i.e. from 39.78 to 47.67% (while in the genuine samples the range was from 2.92 to 6.62%). The same inverted ratio was observed for the β-pinene enantiomers, with values for the dextrorotatory enantiomers ranging from 2.03 to 11.56%, greatly below those of the genuine samples (78.56 to 88.03%). The same difference was observed also for linalool: the (-)-linalool enantiomer was found at higher amount (> 66%) in all the commercial samples with respect to the genuine samples (<42.24%). The enantiomeric ratio of (-)-limonene was similar for samples 1-5 (> 80%), while in the other cases very low ratios were observed (<3.31%). Those values were in all cases outside the characteristic ranges of the genuine samples. Most of the reconstituted samples did not present α-terpineol, apart for samples 6, 10-14 and 16 where it was present practically in a racemic form. Selina-4(15), 7(11) and -3, 7(11) diene were not detected in all the reconstituted samples while the enantiomeric ratio of caryophyllene oxide was in agreement with the genuine oils range. Finally, (E)-β-caryophyllene was determined only in the levorotatory form. Concerning the $\delta^{13}C$ ratios, for most of the components the values were in agreement with the isotopic data obtained for the genuine samples, apart for (E)-β-caryophyllene and caryophyllene oxide, which were both more negative. The latter evidence suggests the possible addition of exogenous (E)-β-caryophyllene to the commercial samples, as one of the major oil terpenes. Such a hypothesis also gives a rationale for the more negative values determined for caryophyllene oxide, being it produced upon oxidation of (E)-β-caryophyllene.

4. Conclusions

In this research, the enantiomeric and isotopic ratios of main terpene constituents of different varieties of *Cannabis Sativa* L. oils were determined, for the first time. An MDGC instrumentation and method were implemented, exploiting a combination of apolar (^{1}D) and chiral stationary phases (^{2}D), with parallel MS and IRMS detection. The coupling of two separation mechanisms allowed, at first instance, for resolving most co-elutions observed in a monodimensional analysis performed on any of the two columns. A more in-depth analysis of the results revealed also the higher accuracy of the data detected/measured by the multidimensional approach, as a consequence of the increased peak separation.

The analysis of a set of commercial oil samples in some cases evidenced enantiomeric and $\delta^{13}C$ ratios outside the typical ranges of genuine oils. Such findings suggest the usefulness of the Es-MDGC-C-IRMS/qMS method, as an effective tool to ascertain the genuineness and quality of these samples. Current efforts are devoted to expand the dataset of oil samples investigated, so to increase the statistical confidence in the genuinity ranges established for the key oil components.

Funding: The authors received no financial support for the research, authorship, and/or publication of this article.

Declarations

Conflicts of Interest/Competing Interests: Co-authors Lorenzo Cucinotta, Gemma De Grazia, Giuseppe Micalizzi, Luana Bontempo, Federica Camin and Danilo Sciarrone declare no conflict of interest. Co-author Luigi Mondello is editor of this journal but was not involved in the peer review of this article.

Ethics approval: Not applicable.

Source of biological material: Not applicable.

Statement on animal welfare: Not applicable.

References

[1] https://eur-lex.europa.eu/LexUriServ/LexUriServ.do?uri=OJ:L:2013:347:0608:0670:IT:PDF

[2] Sommano SR, Chittasupho C, Ruksiriwanich W, Jantrawut P. The Cannabis Terpenes. Molecules. 2020. https://doi.org/10.3390/molecules25245792

[3] Ternelli M, Brighenti V, Anceschi L, Poto M, Bertelli D, Licata M, Pellati F. Innovative methods for the preparation of medical Cannabis oils with a high content of both cannabinoids and terpenes. J Pharm Biomed Anal. 2020. https://doi.org/10.1016/j.jpba.2020.113296

[4] Fiorini D, Scortichini S, Bonacucina G, Greco NG, Mazzara E, Petrelli R, Torresi J, Maggi F, Cespi M. Cannabidiol-enriched hemp essential oil obtained by an optimized microwave-assisted extraction using a central composite design. Ind Crops Prod. 2020. https://doi.org/10.1016/j.indcrop.2020.112688

[5] Micalizzi G, Alibrando F, Vento F, Trovato E, Zoccali M, Guarnaccia P, Dugo P, Mondello L. Development of a Novel Microwave Distillation Technique for the Isolation of *Cannabis sativa* L. Essential Oil and Gas Chromatography Analyses for the Comprehensive Characterization of Terpenes and Terpenoids, Including Their Enantio-Distribution. Molecules. 2021. https://doi.org/10.3390/molecules26061588

[6] Mondello L, Costa R, Sciarrone D, Dugo G. The chiral compound of citrus oils. In: Citrus Oils. Composition, Advanced Analytical Techniques, Contaminants, and Biological Activity; Dugo, G, Mondello, L, editors; CRC Press Taylor & Francis Group: Boca Raton, FL, USA, 2010. pp. 349–403

[7] Dugo P, Ragonese C, Russo M, Sciarrone D, Santi L, Cotroneo A, Mondello L. Sicilian lemon oil: Composition of volatile and oxygen heterocyclic fractions and enantiomeric distribution of volatile components. J Sep Sci. 2010. https://doi.org/10.1002/jssc.201000578

[8] Mondello L, Casilli A, Tranchida PQ, Sciarrone D, Dugo P, Dugo G. Analysis of allergens in fragrances using multiple heart-cut multidimensional gas chromatography-mass Spectrometry. LC-GC Europe 2008; 21(3): 130–7

[9] Bonaccorsi I, Sciarrone D, Cotroneo A, Mondello L, Dugo P, Dugo G. Enantiomeric distribution of key volatile components in Citrus essential oils. Rev Bras Farmacogn. 2011. https://doi.org/10.1590/S0102-695X2011005000123

[10] Do TKT, Hadji-Minaglou F, Antoniotti S, Fernandez X. Authenticity of essential oils. Trends Anal Chem. 2015. https://doi.org/10.1016/j.trac.2014.10.007

[11] Sciarrone D, Schepis A, Zoccali M, Donato P, Vita F, Creti D, Alpi A, Mondello L. Multidimensional Gas Chromatography Coupled to Combustion-Isotope Ratio Mass Spectrometry/Quadrupole MS with a Low-Bleed Ionic Liquid Secondary Column for the Authentication of Truffles and Products Containing Truffle. Anal Chem. 2018. https://doi.org/10.1021/acs.analchem.8b00386

[12] Zhang L, Kujawinski DM, Federherr E, Schmidt TC, Jochmann MA. Caffeine in Your Drink: Natural or Synthetic? Anal Chem. 2012. https://doi.org/10.1021/ac203197d

[13]Reay MK, Knowles TDJ, Jones DL, Evershed RP. Development of Alditol Acetate Derivatives for the Determination of ^{15}N-Enriched Amino Sugars by Gas Chromatography–Combustion–Isotope Ratio Mass Spectrometry. Anal Chem. 2019. https://doi.org/10.1021/acs.analchem.8b04838

[14] Mosandl A, Hener U, Georg Schmarr H, Rautenschlein M. Chirospecific flavor analysis by means of enantioselective gas chromatography, coupled on-line with isotope ratio mass spectrometry. J High Resolut Chromatogr. 1990. https://doi.org/10.1002/jhrc.1240130722

[15] Silfer JA, Engel MH, Macko SA, Jumeau EJ. Stable carbon isotope analysis of amino acid enantiomers by conventional isotope ratio mass spectrometry and combined gas chromatography/isotope ratio mass spectrometry. Anal Chem. 1991. https://doi.org/10.1021/ac00004a014

[16] Mosandl A. Enantioselective capillary gas chromatography and stable isotope ratio mass spectrometry in the authenticity control of flavors and essential oils. Food Rev Int. 1995. https://doi.org/10.1080/87559129509541063

[17] Badea SL, Danet AF. Enantioselective stable isotope analysis (ESIA) — A new concept to evaluate the environmental fate of chiral organic contaminants. Sci Total Environ. 2015. https://doi.org/10.1016/j.scitotenv.2015.01.082

[18] Reichert S, Fischer D, Asche S, Mosandl A. Stable isotope labelling in biosynthetic studies of dill ether, using enantioselective multidimensional gas chromatography, online coupled with isotope ratio mass spectrometry. Flavour Fragr J. 2000; 15: 300-8

[19] Matucha M, Jockisch W, Verner P, Anders G. Isotope effect in gas—liquid chromatography of labelled compounds. J Chromatogr A. 1991. https://doi.org/10.1016/0021-9673(91)85030-J

[20] Cucinotta L, De Grazia G, Salerno TMG, Donnarumma D, Donato P, Sciarrone D, Mondello L. Overcoming the lack of reliability associated to monodimensional gas chromatography coupled to isotopic ratio mass spectrometry data

by heart-cut two-dimensional gas chromatography. J Chromatogr A. 2021. https://doi.org/10.1016/j.chroma.2021.462473

[21] Tranchida PQ, Sciarrone D, Dugo P, Mondello L. Heart-cutting multidimensional gas chromatography: A review of recent evolution, applications, and future prospects. Anal Chim Acta. 2012. https://doi.org/10.1016/j.aca.2011.12.015

[22]https://ec.europa.eu/food/plant/plant_propagation_material/plant_variety_catalogues_databases/search/public/index.cfm?event=SearchVariety&ctl_type=A&species_id=240&variety_name=&listed_in=0&show_current=on&show_deleted

[23] Bicchi C, Binello A, D'Amato A, Rubiolo P. Reliability of Vanden Dool Retention Indices in the Analysis of Essential Oils. J Chromat Sci. 1999. https://doi.org/10.1093/chromsci/37.8.288

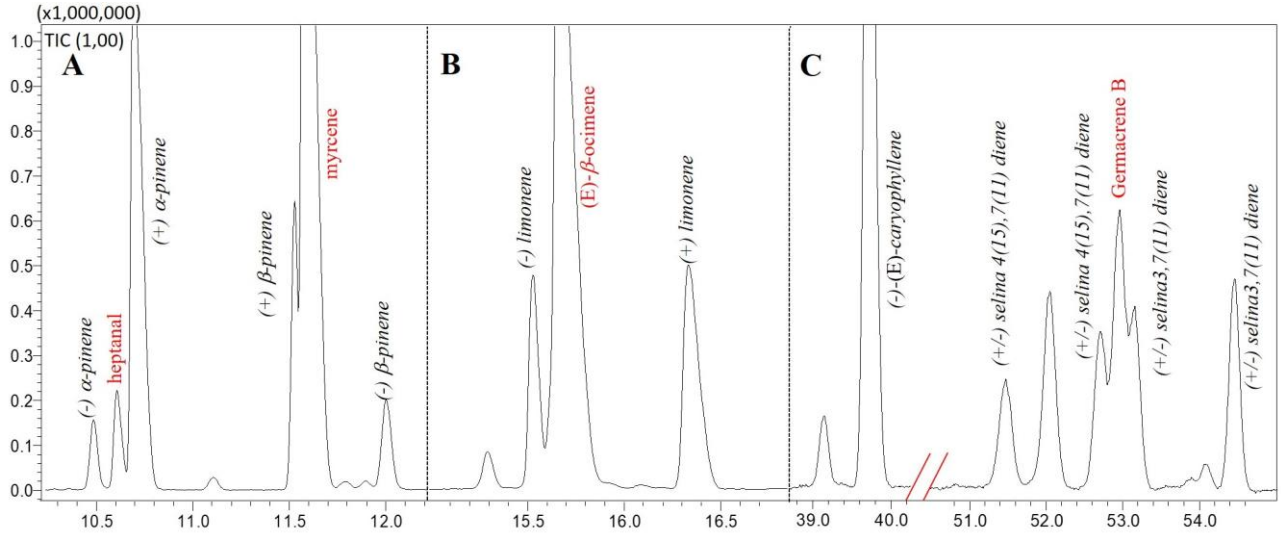


Fig. 1: *Es-GC-C-IRMS/qMS analysis showing the co-elutions of: (+)–α-pinene and (+)–β-pinene peaks (A) and (-)-limonene peak (B) in a Futura 75 essential oil, the enantiomers of selina diene isomers in a Kompolti essential oil (C)*

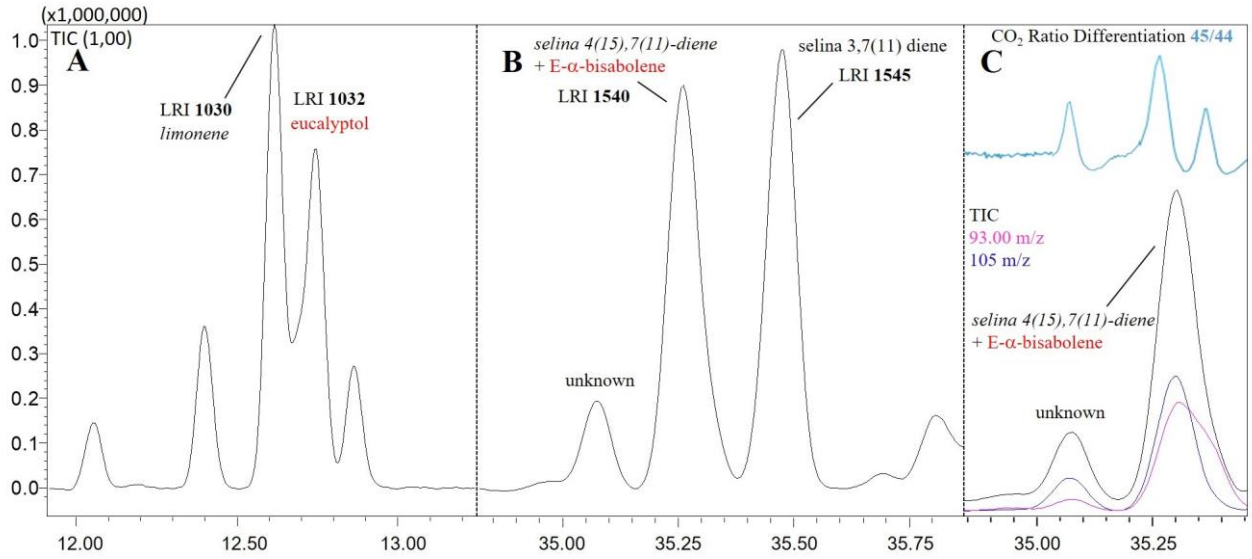


Fig. 2: *GC-C-IRMS/qMS analysis showing the co-elutions of: limonene and eucalyptol peaks (A) and selina 4-(15), 7(11)-diene and (E)-α-bisabolene peaks (B) in a Futura 75 essential oil.* $^{45/44}CO_2$ *ratio differentiation (IRMS: upper trace) and extracted ion chromatogram (qMS: lower traces) of selina 4-15, 7(11)-diene peak (C)*

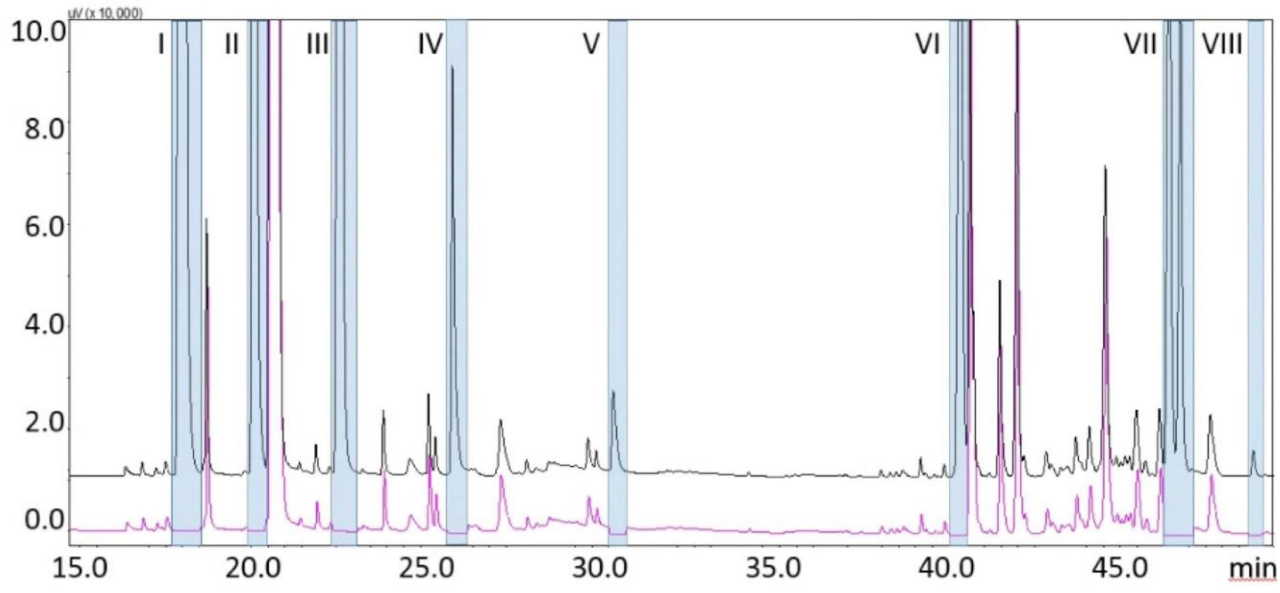


Fig 3. *^{1}D stand-by (black chromatogram) and cut (pink chromatogram) FID analysis of a Cannabis Sativa L. essential oil. Cut windows: I: α-pinene, II: β-pinene, III: limonene, IV: linalool, V: α-terpineol, VI: (E)-β-caryophyllene, VII: selina 4(15),7-11-diene and selina 3,7(11)-diene, VIII:* (E)-*β-caryophyllene oxide*

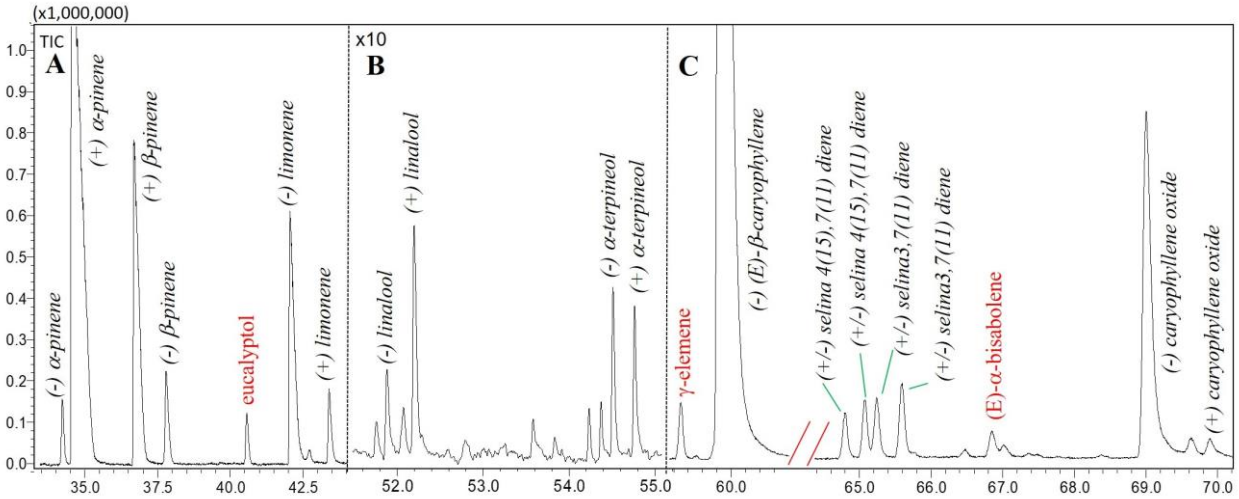


Fig. 4. *MDGC profile of the target monoterpenes in a Futura 75 (A) and a Felina 32 (B) essential oil samples and of the target sesquiterpenes in a Futura 75 essential oil sample (C)*

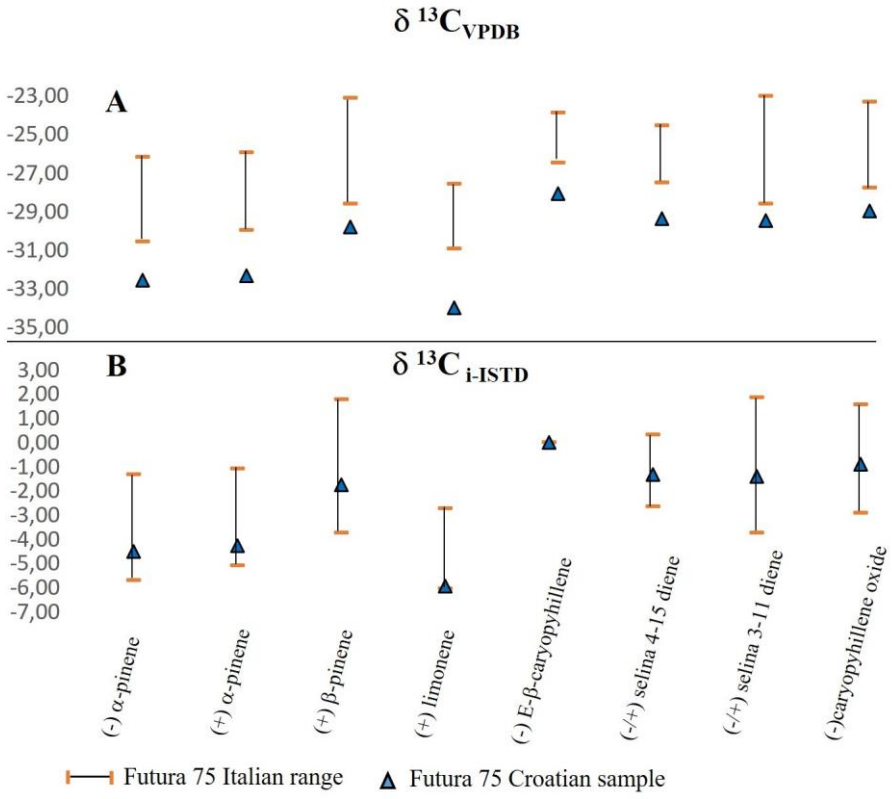
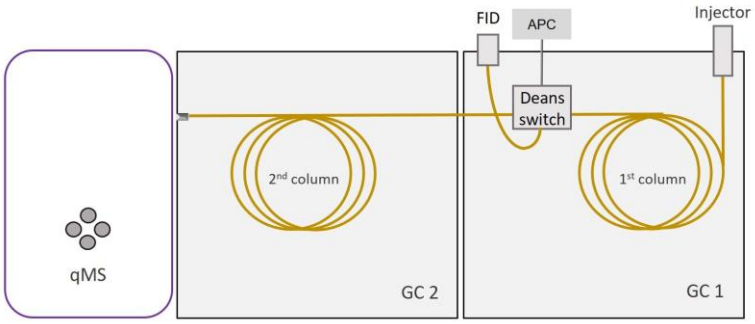


Fig. 5. *(A) Comparison between Italian Futura 75 $\delta^{13}C_{VPDB}$ range (samples 1-9) and Croatian Futura 75 sample (sample 10); (B) comparison after the employment of an isotopic-ISTD*



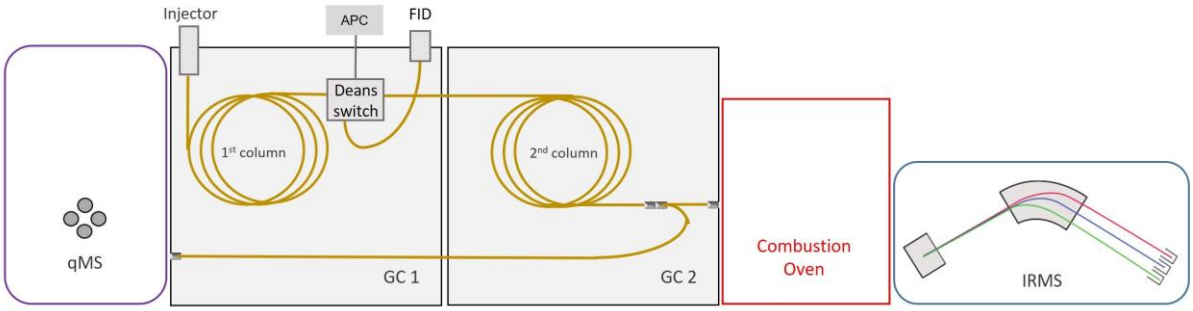
520

521 **Online resource 1**. Scheme of a double-oven MDGC-FID/qMS instrument.

522

523

524

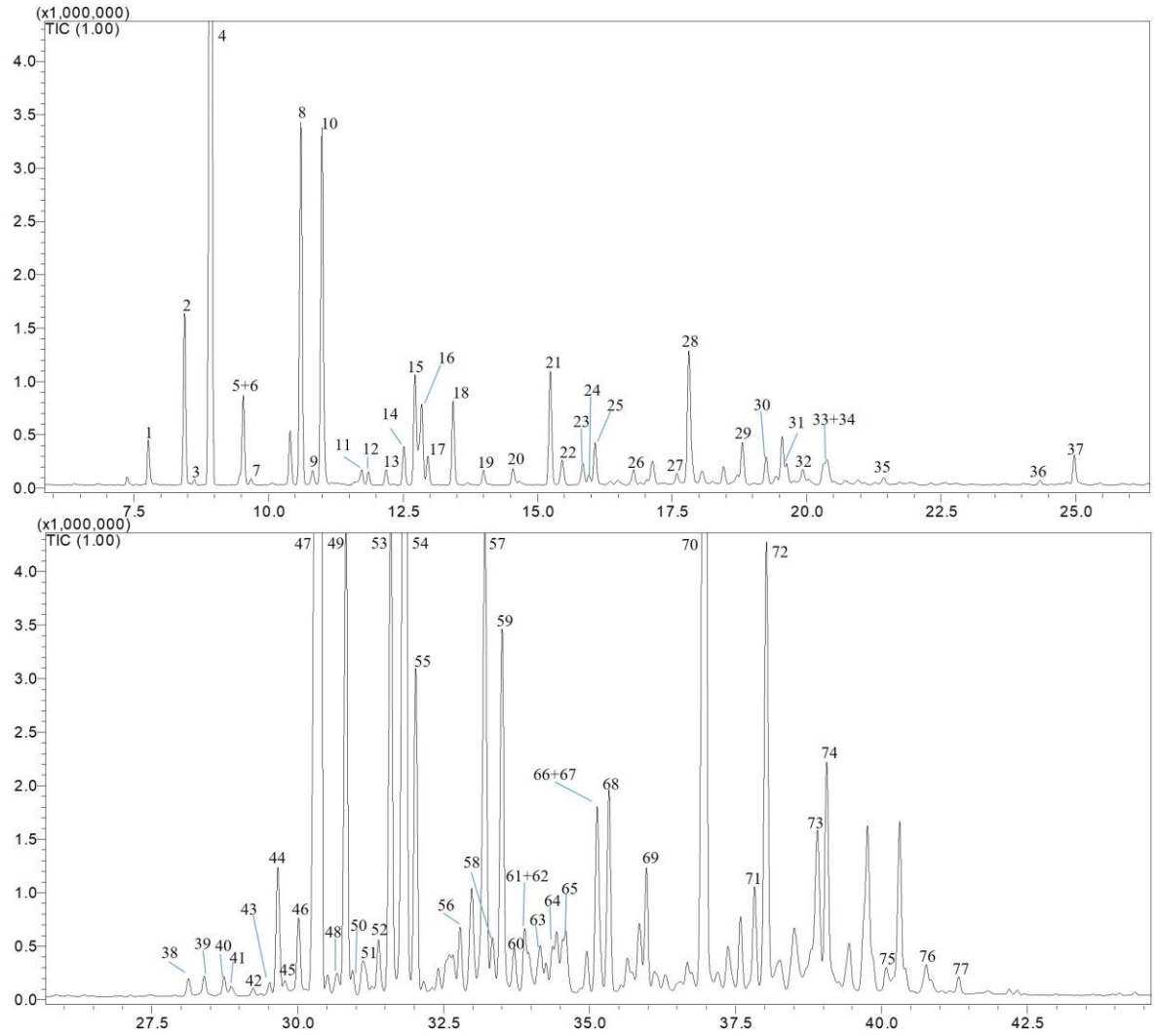


525

526 **Online resource 2**. Scheme of a double-oven MDGC-C-IRMS/qMS instrument.

527

528



Online resource 3: GC-MS chromatogram of a *Cannabis sativa* L essential oil sample. For peak identification refer to Table S1 in supporting information

ID	Name	LRI_{exp}	LRI_{ref}	ID	Name	LRI_{exp}	LRI_{ref}
1	Heptanal	906	902	40	Hexyl-Hexanoate	1385	1390
2	Hashishene	921	921	41	7-epi-Sesquithujene	1387	1387
3	α-Thujene	925	927	42	Sativene	1396	1394
4	α-Pinene	933	933	43	α-Funebrene	1402	1403
5	α-Fenchene	950	950	44	β-Longipinene	1406	1405
6	Camphene	950	953	45	α-Gurjunene	1408	1406
7	Thuja-2,4(10)-diene	953	953	46	α-, (Z)-Bergamotene	1414	1416
8	β-Pinene	978	978	47	(E)-Caryophyllene	1421	1424
9	6-methyl-Hept-5-en-2-one	984	986	48	γ-Elemene	1430	1432
10	Myrcene	988	991	49	α-, (E)-Bergamotene	1434	1432
11	α-Phellandrene	1007	1007	50	α-Guaiene	1436	1438
12	δ-3-Carene	1010	1009	51	Aromadendrene	1441	1438
13	α-Terpinene	1017	1018	52	(E)-Geranylacetone	1447	1450
14	*p*-Cymene	1024	1025	53	(E)-, β-Farnesene	1452	1452
15	Limonene	1029	1030	54	α-Humulene	1458	1454
16	Eucalyptol	1032	1032	55	9-epi-(E)-Caryophyllene	1462	1464
17	(Z)-β-ocimene	1035	1035	56	α-Curcumene	1480	1480
18	(E)-β-ocimene	1045	1046	57	β-Selinene	1491	1492
19	γ-Terpinene	1058	1058	58	Valencene	1495	1492
20	(Z)-Sabinene hydrate	1070	1069	59	α-Selinene	1498	1501
21	Terpinolene	1086	1086	60	α-Bulnesene	1503	1505
22	*p*-Cymenene	1091	1093	61	β-Bisabolene	1508	1508
23	Linalool	1100	1101	62	β-curcumene	1510	1511
24	(E)-Sabinene hydrate	1102	1099	63	γ-Cadinene	1515	1512
25	Nonanal	1104	1107	64	δ-Cadinene	1520	1518
26	Fenchyl alcohol	1120	1119	65	β-Sesquiphellandrene	1524	1523
27	*p*-Mentha-2,8-dien-1-ol	1137	1138	66	Selina-4(15),7(11)-diene	1540	1540
28	(E)-Pinocarveol	1142	1141	67	(E)-, α-Bisabolene	1540	1540
29	Pinocarvone	1163	1164	68	Selina-3,7(11)-diene	1544	1546
30	Borneol	1173	1173	69	(E)-Nerolidol	1561	1561
31	Terpinen-4-ol	1181	1184	70	Caryophyllene oxide	1585	1587
32	*p*-Cymen-8-ol	1188	1189	71	Fokienol	1600	1596
33	α-Terpineol	1196	1195	72	Humulene epoxide II	1614	1613
34	Myrtenol	1198	1202	73	Caryophylla-4(12),8(13)-dien-5-β-ol	1638	1636
35	(E)-Carveol	1220	1223	74	Caryophylla-4(12),8(13)-dien-5-α-ol	1641	1642
36	Bornyl Acetate	1284	1285	75	Intermedeol	1668	1668
37	Tridecane	1298	1300	76	α-bisabolol	1686	1688
38	α-Ylangene	1370	1371	77	Juniper camphor	1701	1696
39	α-Copaene	1377	1375				

Online resource 4. Peak identification obtained from the GC-MS analysis (Online material 3) of a *Cannabis sativa* L. essential oil